UNIVERSITY OF LEEDS

This is a repository copy of *Polycrystalline SrTiO3 thin film grown by pulsed laser deposition on a (111) oriented platinum seed layer*.

White Rose Research Online URL for this paper:
https://eprints.whiterose.ac.uk/181614/

Version: Published Version

Monograph:

Shepley, P orcid.org/0000-0003-1240-593X (2020) Polycrystalline SrTiO3 thin film grown by pulsed laser deposition on a (111) oriented platinum seed layer. Report. Materials from the Royce Deposition System (6). University of Leeds

10.48785/100/85

White Rose
university consortium
Universities of Leeds, Sheffield & York

eprints@whiterose.ac.uk
https://eprints.whiterose.ac.uk/

Polycrystalline SrTiO$_3$ thin film grown by pulsed laser deposition on a (111) oriented platinum seed layer

P.M. Shepley

This application note describes the growth and characterisation of a polycrystalline SrTiO$_3$ thin film grown in the Royce Deposition System by pulsed laser deposition. The film was characterised by X-ray reflectivity and diffraction and impedance spectrocopy.

1 Introduction

SrTiO$_3$ (STO) is perovskite crystal [1] with applications in capacitors and as a gate barrier. At room temperature bulk STO has a relativite dielectric constant (relativity permittivity) of $\varepsilon_r \approx 300$. The dielectric properties of STO thin films can vary compared to the bulk [1–3]. Applications of thin film STO usually require a high permittivity.

2 Growth

The STO film was deposited by pulsed laser deposition (PLD) in the Royce Deposition System. The target was mounted below the substrate with a target-substrate distance of 55 mm and was scanned during ablation at a speed of 2.5 mm/s. The base pressure of the system was to 2.9 x10^{-9} mbar. O$_2$ gas was flowed through the chamber at 10 sccm with the main gate valve to the turbo pump closed and a bypass butterfly valve controlled by a feedback loop to maintain an equilibrium process pressure of 0.1 mbar. The STO film was deposited onto a 19 nm thick, (111) textured sputtered Pt film on a glass. The substrate was heated to 600 °C at a rate of 5 °C/minute. A pyrometer set to an emissivity of 0.2 (the lowest value available) gave the temperature of the Pt surface as 694 °C prior to STO deposition. A KrF excimer laser with a wavelength of 248 nm was used to ablate the target. The fluence was measured before deposition as 1.55 J/cm^2. The target was cleaned with a pre-ablation of 3000 pulses at a repetition rate of 5 Hz, then the shutter was opened and STO was deposited onto the substrate using 6600 laser pulses at a repetion rate of 5 Hz. After growth a pyrometer set to an emissivity of 0.8 (an estimated value for STO) gave the temperature of the STO surface as 590 °C. The sample was cooled at 5 °C/minute in 0.1 mbar of oxygen.
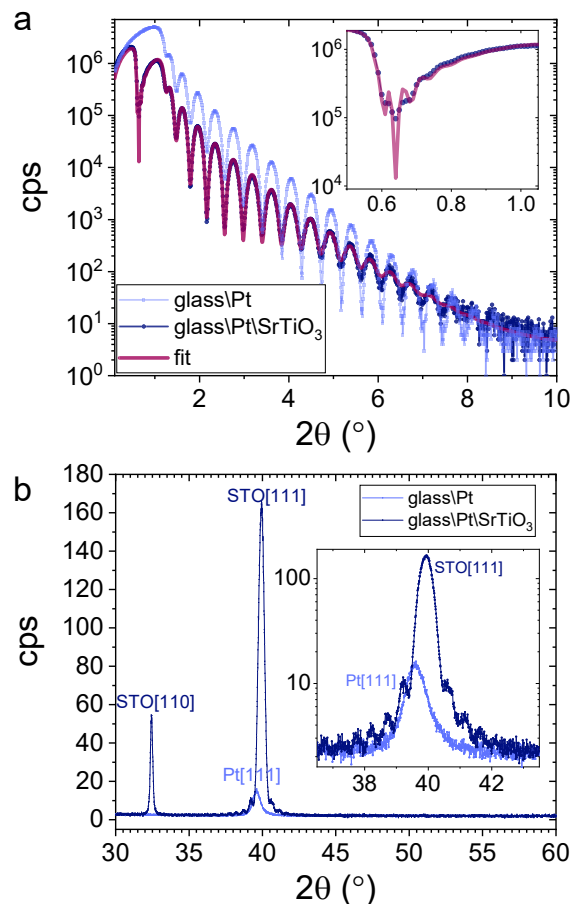

Figure 1: a) X-ray reflectivity data of the Pt seed layer before STO deposition, X-ray reflectivity data of the STO thin film and a GenX fit to the STO film data. The inset is an enlarged area at low angle showing Kiessig fringes from the STO film thickness. b) X-ray diffraction data of the STO thin film on a Pt seed layer and of the Pt seed layer before STO deposition. The inset shows a enlarged plot of the (111) peaks on a logarithmic scale.

3 Properties

3.1 Structural Properties

The STO thin film was measured using X-ray reflectivity (XRR) and X-ray diffraction (XRD) in a Bruker D8 diffractometer in Bragg-Brantano geometry with a $Cu_{K\alpha}$ source ($\lambda = 1.5406$ Å).

Figure 1 shows the XRR of the STO thin film. The XRR data was fitted with GenX [4]. The fit gave an STO thickness of 909 Åand an average surface roughness of 55 Å. The fitted parameters are shown in Table 1.

The XRR signal of the Pt seed layer on glass is still present after STO deposition. Figure 1a shows XRR scans of the sample before and after growth of the STO film. After growth of the STO film the Kiessig finges and critical edge due to the Pt seed layer are still prominent features. The scattering length density of the Pt is much higher than that of the STO, which allows critical edges due to both materials to be present in the XRR scan. Figure 1b shows the GenX fit of the XRR data for the STO sample, which shows that the two critcal edge features can be fitted with the reflectivity model. The inset in Figure 1b is an enlarged section of the fitted STO data between the two critical edges, where Kiessig fringes from the STO film thickness are visable.

Figure 1 shows the XRD of the STO thin film and the Pt seed layer before STO deposition. Both the (110) and (111) STO peaks are present in the XRD spectrum, showing that the film is polycrystalline. The peak positions are consistent with a perovskite crystal structure.

The Scherrer equation was used to estimate the size crystallites in the film. The equation for crystallite size is given by

$$D = \frac{K\lambda}{FWHM(2\theta)\cos\theta}, \qquad (1)$$

where θ is the Bragg angle of the peak in radians, $FWHM(2\theta)$ is the full width half maximum in 2θ (radians), λ is the wavelength of the incident X-rays and K is a dimensionless parameter relating to the shape of the crystallites [5] (0.8540 for the (110) peak and 0.8551 for the (111) peak. The Scherrer equation gives a crystallite size of $D = 258 \pm 2$Å for the (110) peak and $D = 146.9 \pm 0.4$Å for the (111) peak. The size of the crystallites in the STO film is between 16 and 28 % of the film thickness.

GenX fitting parameter	Value
Thickness - SrTiO$_3$ (Å)	909
Density - SrTiO$_3$ (% of bulk)	100
Roughness - SrTiO$_3$ (Å)	55
Thickness - Pt (Å)	192
Density - Pt (% of bulk)	100
Roughness - Pt (Å)	4
Roughness - glass (Å)	6

Table 1: Structural parameters obtained by fitting XRR data with GenX.

3.2 Electrical Properties

The room temperature electrical properties of the film were measured using a Solartron impedance analyser. An array of Pt electrodse were added to the top of the STO film by sputter deposition so that probes could contact the top and bottom of the film for impedance and capacitance measurements. The top electrode used to make measurements was 250 μm in diameter. A sinusoidally varying voltage of 100 mV (rms) was applied across the film a the frequency range of 0.1 Hz to 1 MHz.

Complex impedance data are plotted in Figure 2. Figure 2a shows the real (Z') and imaginary (Z") fitted to an equation describing the simple RC circuit in Figure 4. The complex impedance is given by

$$Z(\omega) = Z'(\omega) + ßZ''(\omega), \qquad (2)$$

where for the circuit shown in Figure 4

$$Z'(\omega) = R_S + \frac{R_1}{1 + \omega^2 R_1^2 C_1^2}, \qquad (3)$$

and

$$Z''(\omega) = \frac{\omega R_1^2 C_1}{1 + \omega^2 R_1^2 C_1^2}, \qquad (4)$$

where ω is the angular frequency $\omega = 2\pi f$, R_s and R_1 are resistances and C_1 is a capacitance. The parameters R_s,R_1 and C_1 extracted from the fit to the real impedance versus frequency, along with the calculated dc resistance R_{dc} and resistivity are given in Table 2.

The value for C_1 is consistent with the measured capacitance of the film, which lies within the range 1.5 to 2.5 nF for frequencies from 1 Hz to 1 MHz (Figure 3a). The fit to the imaginary data yields values of
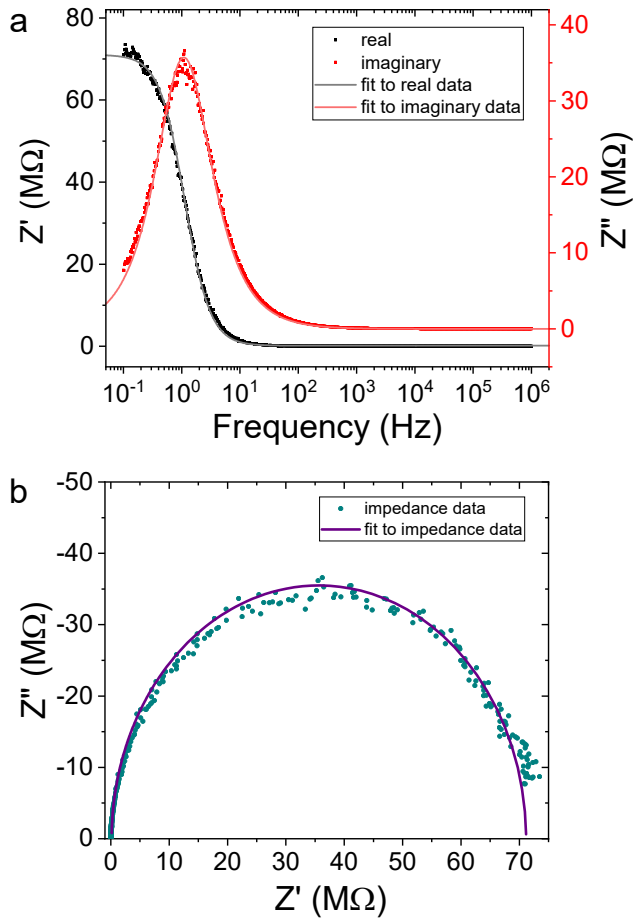
Figure 2: Complex impedance data of the STO thin film with Pt electrodes. a) Real (Z') and imaginary (Z") parts of the impedance plotted against input voltage frequency. The solid lines are fits a simple RC circuit model. b) The imaginary part of the impedance plotted against the real part of the impedance. The solid lines are calculated using the fits in a).
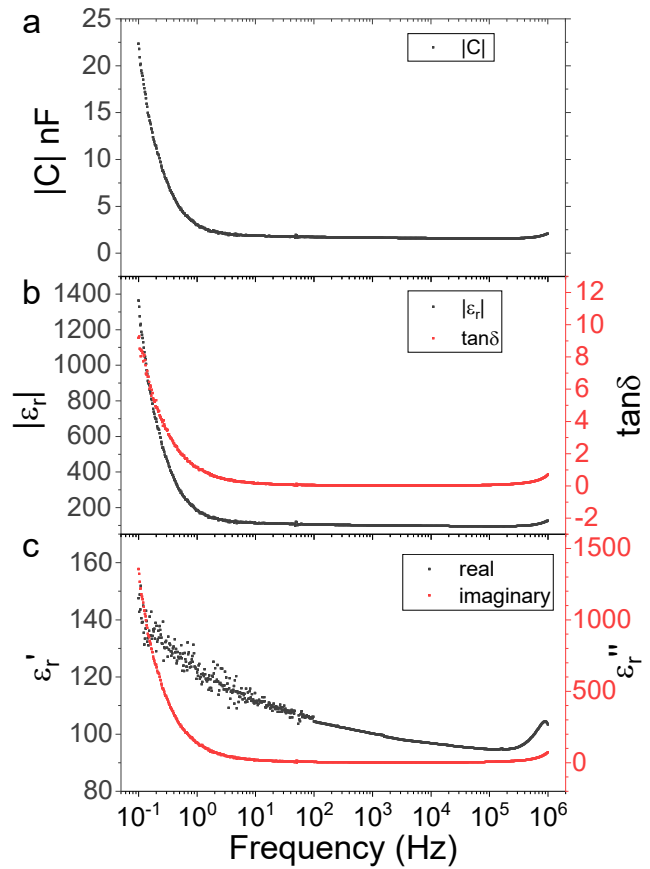

Figure 3: Capacitance and relative permittivity data of the STO thin film with Pt electrodes. a) Magnitude of the capacitance plotted against input voltage frequency. b) Magnitude of the relative permittivity and the loss tangent plotted against input voltage frequency. c) Real (ε') and imaginary (ε'') parts of the relative permittivity plotted against input voltage frequency.

Parameter or property	Value
R_s (MΩ)	0.15$\pm$0.03
R_1 (MΩ)	70.88$\pm$0.09
C_1 (nF)	1.998$\pm$0.005
R_{dc} (MΩ)	71.03$\pm$0.09
ρ (GΩcm)	3.8$\pm$0.3
σ (pS/cm)	2.6$\pm$0.2

Table 2: Electrical parameters obtained by fitting complex impedance data in Figure 2 to Equations 3 and 4 and properties (resistivity ρ and conductance σ calculated using the fitted parameters.
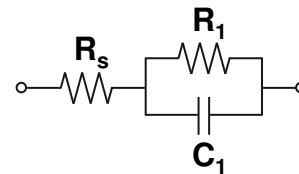

Figure 4: A simple RC circuit used to model the impedance of the thin film.

R_1 and C_1 that are consistent with the fit to the real impedance.

In Figure 2b the impedance data have been plotted as Z'' versus Z' and fit parameters from Figure 2a have been used to plot a fit line. The single semicircular shape of the curve suggests that one conduction mechanism dominates. In this plot the dc resistance is the intercept with the x axis at 71 MΩ.

The capacitance, loss tangent and relative permittivity are shown in Figure 3. The size of the relative permittivity is close to 100 for most of the measured frequency range, which is comparable with other thin films of STO [1–3]. The permittivity of STO thin films is much higher than other common gate dielectrics, such as SiO_2 or MgO, which tend to have relative permittivity values of the order of 3 to 10 [6, 7]. The high permittivity of our STO thin films means that they can be effective in thin film capacitors or gated devices.

4   Further Information

The Royce Deposition System is a multichamber, multitechnique thin film deposition tool based at the University of Leeds as part of the Henry Royce Institute. Materials from the Royce Deposition System are available as a facility service and for collaborations.

Sample growth ID:
MET20190613_01, PLD20190618_01

References

1.   S. Krupanidhi *et al.*, *Thin Solid Films* **249**, 100–108 (Sept. 1994).

2.   Y. A. Boikov *et al.*, *Physical Review B - Condensed Matter and Materials Physics* **74**, 7–12 (2006).

3.   T. Suzuki *et al.*, *Integrated Ferroelectrics* **76**, 47–57 (Nov. 2005).

4.   M. Björck *et al.*, *Journal of Applied Crystallography* **40**, 1174–1178 (2007).

5.   J. I. Langford *et al.*, *Journal of Applied Crystallography* **11**, 102–113 (1978).

6.   I.-C. Ho *et al.*, *Journal of Sol-Gel Science and Technology* **9**, 295–301 (Oct. 1997).

7.   S. Holten *et al.*, *Journal of Applied Physics* **90**, 1941–1949 (Aug. 2001).